Corrosion Behavior and Kinetics of Early Stages of Low Alloy Steel under H_2S/CO_2 Environment

Chi Yu[1], Ping Wang[1,], Xiuhua GAO[2]*

[1] The Key Laboratory of Electromagnetic Processing of Materials, Ministry of Education, Northeastern University, Shenyang 110819, China
[2] The State Key Laboratory of Rolling and Automation, Northeastern University, Shenyang 110819, China
[*]E-mail: wping@epm.neu.edu.cn

The corrosion behavior and kinetics of early stages of low alloy steel under H_2S and CO_2 environment is investigated by immersion and electrochemical experiments. Scanning electron microscopy (SEM) and X-ray diffraction (XRD) are employed to reflect the corrosion products and phase compositions. Results indicate that the corrosion products are composed of mackinawite. The numerous mackinawite and complexity compound Fe are observed during immersion 24 h and 48 h, a thin inner layer and an inhomogeneous outer layer have appeared. After immersion 96 h and 192 h, Fe is not observed, the thickness of inner layer and outer layer increase, the corrosion products trend to homogeneous and compact, the mackinawite grows larger and adheres. The absence of $FeCO_3$ suggests that the corrosion process is governed by H_2S corrosion. Finally, the relationship of corrosion surface morphology, phase compositions, corrosion kinetics and electrochemical corrosion parameters are discussed.

Keywords: low alloy steel; corrosion behavior; electrochemical techniques; SEM

1. INTRODUCTION

The corrosion problem of alloy steel for oil and gas industry has attracted more attention, the special environment in the presence of H_2S and CO_2 could induce severe general and localized corrosion [1-3]. It is imaginable that once the alloy steel fails due to corrosion, it will lead to serious accident and huge economic loss. So it is essential to develop a new type of low alloy steel for oil and gas industry and study the corrosion mechanism.

Corrosion is a very complex process, and the behavior of corrosion changes as erosion time extends. Some papers about the early stages of corrosion have been published [4-8]. Guo et al. [6]

studied the initial stages of atmospheric corrosion on interstitial free steel in NaCl electrolyte. Zimer et al. [7] investigated the initial stages of pitting corrosion of AISI 1040 steel in an alkaline sulfide solution. Bai et al. [8] reported the early corrosion stages of API X52 steel exposed to H_2S environments. Although some works have indicated that the early stage of corrosion is very important, papers on the early stages of H_2S and CO_2 corrosion are few, the corrosion process under H_2S and CO_2 environment is still poorly understood. It is well known that the corrosion behavior of alloy steel is an electrochemical process. Therefore, electrochemical measurement is essential to analyze its corrosion properties, the technology has been widely used to investigate the corrosion mechanism and has been proven to be effective [9-16]. Zhang et al [15] investigate the electrochemical characteristics of early corrosion stage of carbon steel, immersion time is 70 h. Zheng et al [16] study the electrochemistry of mild steel corrosion in a mixed H_2S/CO_2 aqueous environment for short term exposures of a few hours, but no considering the corrosion mechanism during the different immersion period.

In this paper, corrosion properties of early stages of alloy steel during the different immersion period are investigated under H_2S/CO_2 coexistence conditions. The experimental are carried out by weight loss tests and electrochemical measurements, including potentiodynamic polarization curves and electrochemical impedance spectroscopy (EIS). The corrosion morphology and phase compositions are characterized by scanning electron microscopy (SEM) and X-ray diffraction (XRD).

2. EXPERIMENTAL

2.1 Materials and sample preparation

Effect of alloy elements on the corrosion resistance is very important. The steel with elements such as C, Si, Mn, P, S and Cr shows the poor mechanical property and corrosion resistance [8]. Liu et al [17] add some alloy elements Al, Ni and Nb, they can improve the strength and toughness. Ref [18] add alloy element Mo, it can make the grain refining and improve the corrosion resistance. Cu is added to the mild steel, it can improve the strength, and exist in the corrosion product films, further improve the corrosion resistance [19]. Park et al [20] and Mishra et al [21] study the effect of W on the corrosion behavior in sulfuric acid, it is found that the corrosion resistance of W steel is very well, which may be result from W can form the WO_4^{2-}, play the role of corrosion inhibitor. Based on the above analysis, a new type of low alloy steel is developed, with a composition (mass, %) of 0.085 wt.% C, 0.24 wt.% Si, 1.36 wt.% Mn, 0.006 wt.% P, 0.002 wt.% S, 0.23 wt.% Cr, 0.16 wt.% Cu, 0.21 wt.% W, 0.21 wt.% Mo, 0.11 wt.% Ni, 0.012 wt.% Nb and Fe balance, is used in this experiment. The tested steel is obtained with rolling parameters including final rolling temperature for 840°C, final cooling temperature for 617°C, cooling rate 15°C/s. The corrosion test specimens are machined into 25 mm×20 mm×4 mm for weight loss test. The electrochemical test samples are cut into 10 mm×10 mm×3 mm, and the exposed surface is 10 mm×10 mm, with an area of 100 mm^2, all other surfaces are isolated from the environment by epoxy resin. Prior to testing, the samples are ground with a series of SiC waterproof abrasive papers (100, 600, 800, 1200 and 1500).

2.2 Experimental process

The immersion experimental is carried out in a 5 L high pressure autoclave. The test solution is 3.5 wt% NaCl (analytical grade reagent) solution. N_2 is bubbled into the electrolyte for 3 h to deoxygenate, and H_2S/CO_2 are purged into the solution for 1 h to saturate the solution. Then, the electrolyte is heated to 75°C and the total pressure is 12 bar with partial pressure 0.9 bar H_2S, 6.4 bar CO_2 and 4.7 bar N_2. Four immersion durations of 24 h, 48 h, 96 h and 192 h are chosen to study the corrosion mechanism of early stages. After immersion tests, the specimens are removed from high pressure autoclave, and rinsed with deionized water. They are divided into two groups: the specimens in group one are descaled (the solution: 50 ml 37% HCl, 5 g hexamethy lenetebramine (urotropine) and 450 ml deionized water), rinsed with water and absolute alcohol, dried in nature state and weighted again with a precise of 0.01mg. The specimens in group two are not descaled, which will be used for corrosion surface and phase compositions analysis. Three parallel samples are used to perform weight loss test, and the mean value is obtained.

The corresponding corrosion rate (v) is calculated according to the following equation [22].

$$v = \frac{8.76 \times 10^4 \times \Delta m}{A \times t \times \rho} \qquad (1)$$

where v is the average corrosion rate, mm/year, Δm is the weight loss, g; A is the exposed surface area of samples, cm^2; t is the immersion duration, h; ρ is the density of tested metal (7.916g/cm^3).

The conversion of gravimetric parameters into electrochemical ones is made by mean of Faraday's law [10].

$$i_{corr} = \frac{nF\Delta m}{MtA} \qquad (2)$$

where i_{corr} is the current density in A/cm^2 which stands for corrosion rate, F is Faraday's constant (96500 coulombs), n is valence, M is molecular weight of tested steel in g/mol, t is the immersion time in s.

The electrochemical measurements are performed by an electrochemical workstation (PATSTAT2273). A conventional three-electrode cell is used for the polarization curves and electrochemical impedance spectroscopy (EIS) experiments. The platinum electrode is used as the auxiliary electrode, the saturated calomel electrode (SCE) is used as the reference electrode, and the sample is used as the working electrode. The polarization curves are recorded potentiodynamic with a scanning rate of 1mV/s and the potential range from 1.2 V to - 0.1 V. The electrochemical impedance spectroscopy experiments are performed by applying a small sinusoidal perturbation (8 mV) to the reaction system, and a frequency range is from 100 kHz to 0.1 Hz. The electrochemical measurements are conducted in aerated 3.5 wt% NaCl containing H_2S and CO_2 at 75°C, the pH of the test solution is 4.21 by actual measurement.

2.3 Surface analysis

The surface morphologies and phase compositions of corrosion product films are analyzed using SEM and X-ray diffraction (XRD) with filtered Cu Kα radiation.

3. RESULTS AND DISCUSSION

3.1 Mass loss measurements

The average corrosion rates are 1.57, 2.34, 1.20 and 0.94 mm/year for samples after immersion time 24, 48, 96, 192 and 288 h, respectively. The mean values of corrosion current density are obtained for 0.136 mA/cm^2, 0.202 mA/cm^2, 0.104 mA/cm^2 and 0.081 mA/cm^2 for immersion time 24 h, 48 h, 96 h and 192 h, respectively. As shown in Fig.1. We can see that the corrosion current density changes as immersion time. At the first stage (before immersion 48 h), corrosion current density increases sharply. At middle stage from 48 h to 96 h, the corrosion current density decrease. After immersion 96 h, the corrosion current density trends to be stable. The polynomial fitting equation by least square method could be expressed as follows.

$$i_w = 3.765 \times 10^{-7} t^3 - 0.0001158 t^2 + 0.008783 t - 0.00329 \tag{3}$$

where the i_w is the average current density in mA/cm^2 and t is immersion time (h). We can solve the all solutions of equation (3), $t_1 = 0.3765$, $t_2 = 134.1146$ and $t_3 = 137.0786$, respectively. So the equation is not suitable for the near zero hour and values between 134.1146 and 137.0786. We collect a few dates, drawing graphics such as Fig.1, the method is proved to be effective. Based on the equations (1) and (2), it is found that the corrosion current density is much more, and the corrosion rate is bigger, it is probable to appear the serious local corrosion.
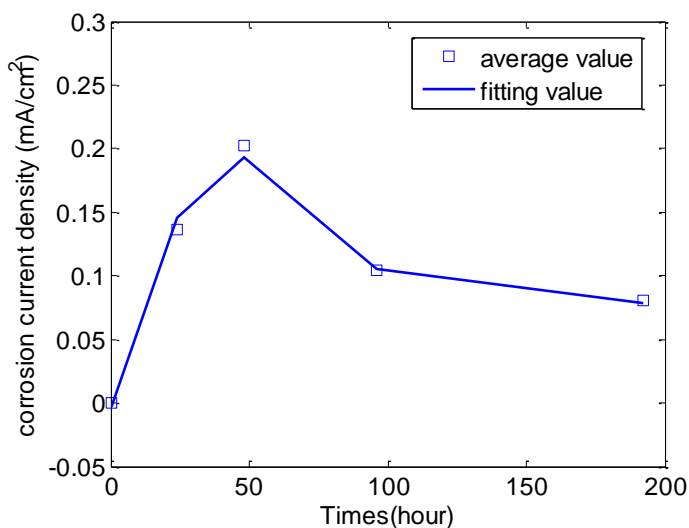
Figure 1. Corrosion current density of tested steel as a function of the immersion time

3.2 Surface morphologies and phase composition analysis of corrosion products

The microscopic corrosion morphology characterizations of tested steel with scale are shown in Fig.2. Obviously, the corrosion products after immersion 24 h and 48h are loose, the gaps are possible to be passages that the corrosion solution diffuses into the inner layer and even into the substrate surface, which may lead to pitting corrosion.
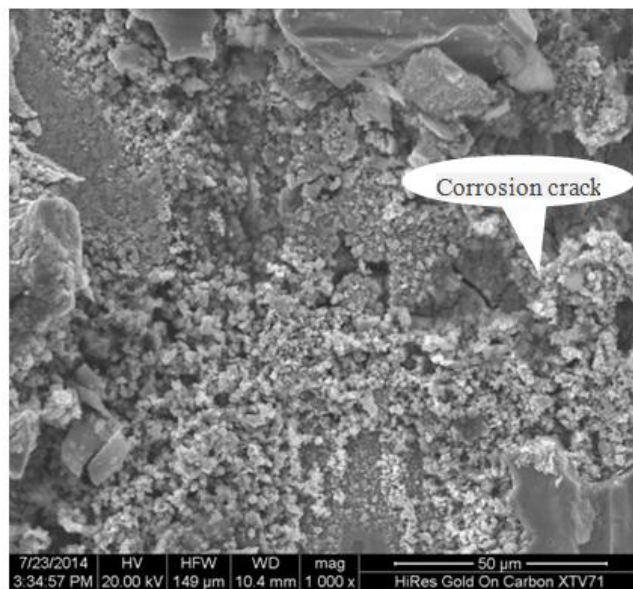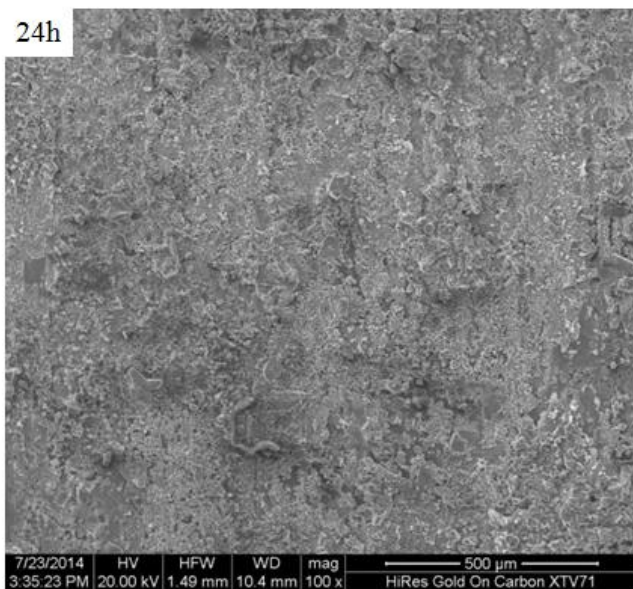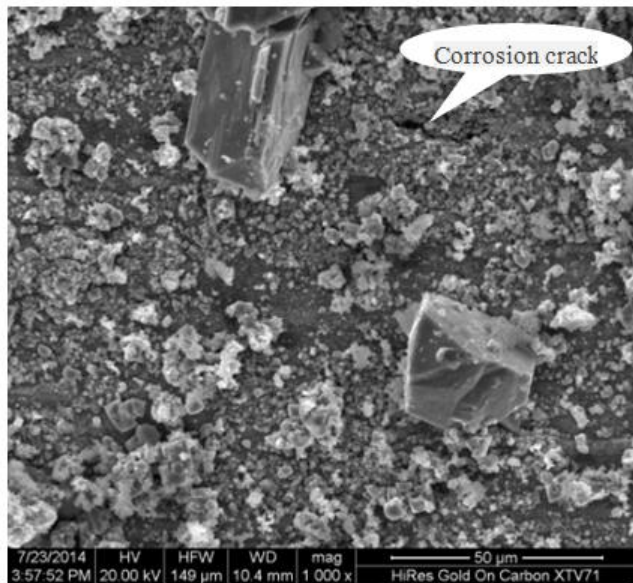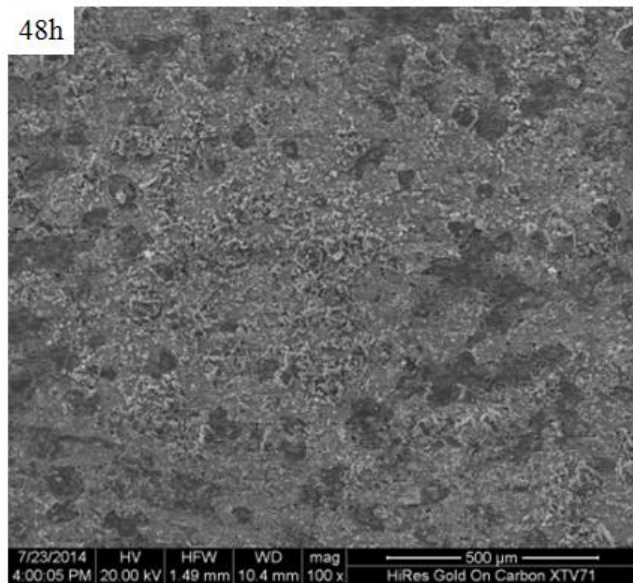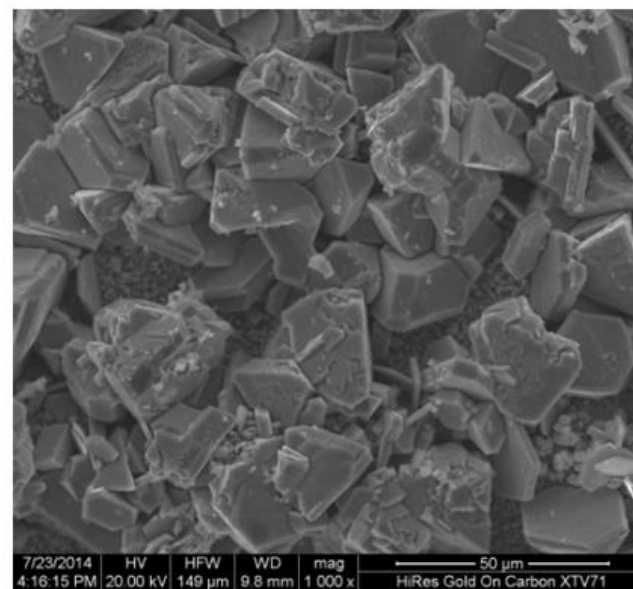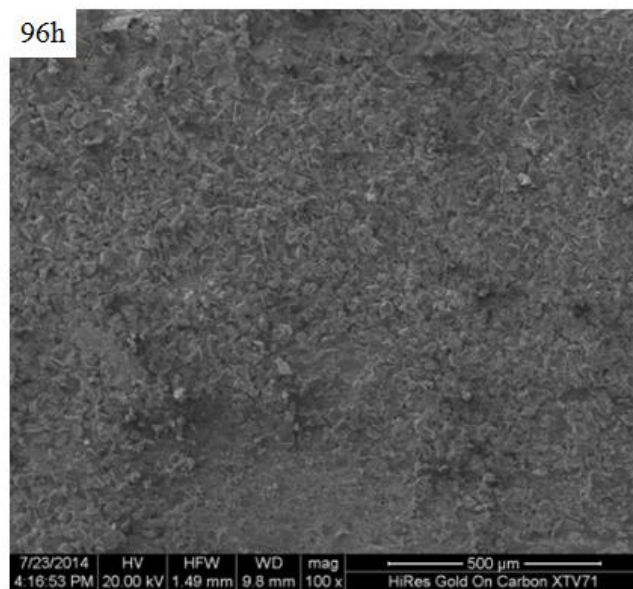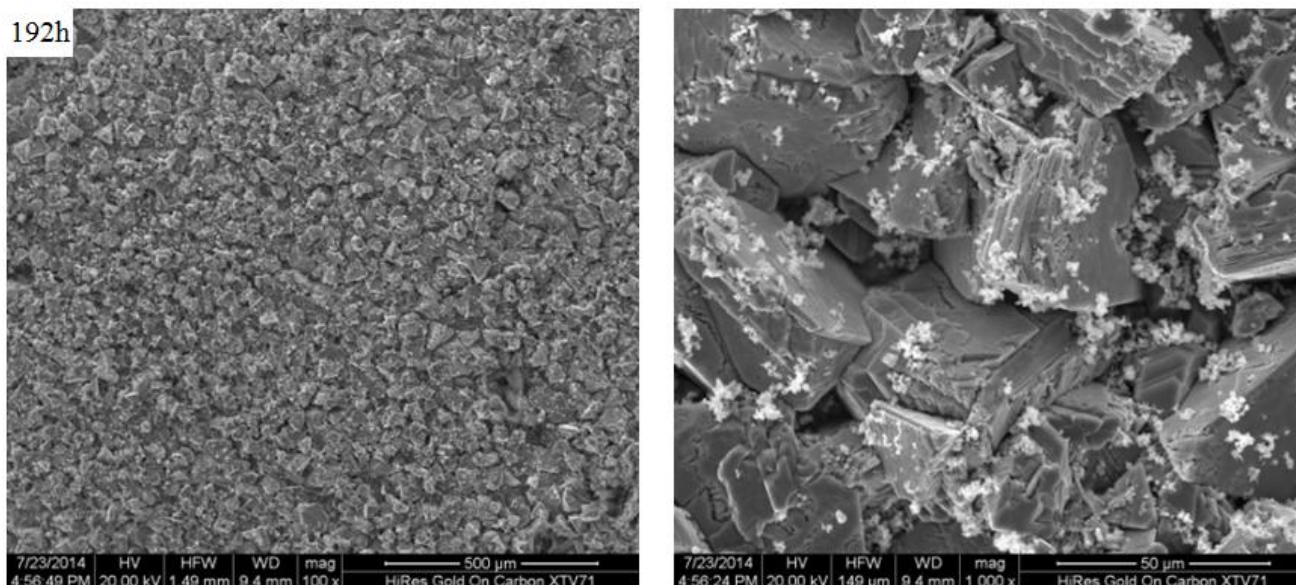
Figure 2. SEM images of corroded surface under different immersion durations:

Comparatively, the corrosion scales produced after immersion 96 h are very compact, it can protect the steel matrix efficiently. When the tested steel is immersed for 192 h, the crystal grains are more regular and dense. The film is more compact and helpful to decrease the corrosion rate. In general, the regular and dense scale can impede the corrosive ions through the scale, it is a well protection for the steel matrix. The analytic results are in is consistent with the weight loss tests.

The phase compositions of tested steel after immersion 48 h and 96 h are shown in Fig.3. It can be seen that the corrosion products are comprised of mackinawite, the absence of $FeCO_3$ in the corrosion scales indicates that the H_2S corrosion has a significant effect on the whole reaction process and iron sulfide is superior to precipitating on the steel surface compared with iron carbonate [8, 23-25]. Only Fe is remained when immersed time for 24h and 48h, the result may be attributed to the thin corrosion films are formed, because only a few corrosion products appear at this time. When immersion time is 96 h and 192 h, Fe is not detected; the mackinawite grows and adheres, which will increase the thickness of corrosion product films.
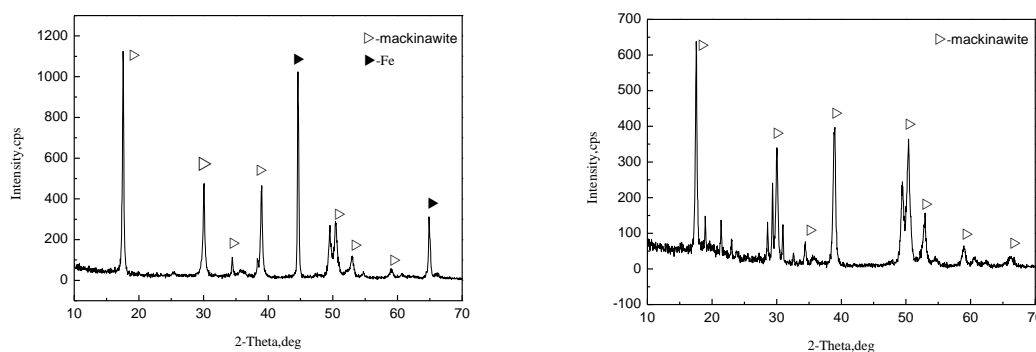
Figure 3. XRD pattern of the coupons of different immersion durations

Fig.4 shows cross section morphology characterization. A loose inner layer about 2-5 μm and a porous outer layer ranging from 0 μm to 5 μm are formed on the coupon surface of 24 h immersion. After immersion 48 h, the inner layer is damaged, a discontinuous inner layer is attached on the steel substrate. With immersion time goes by from 96 h to 192 h, the thickness of the inner layer grow. It is seen that the inner layer of coupons is more compact, a denser inner layer has formed. That acts as a shield to resist eroding further. Outer layer of coupons after immersion 192 h is thicker than one of 96h immersion duration.
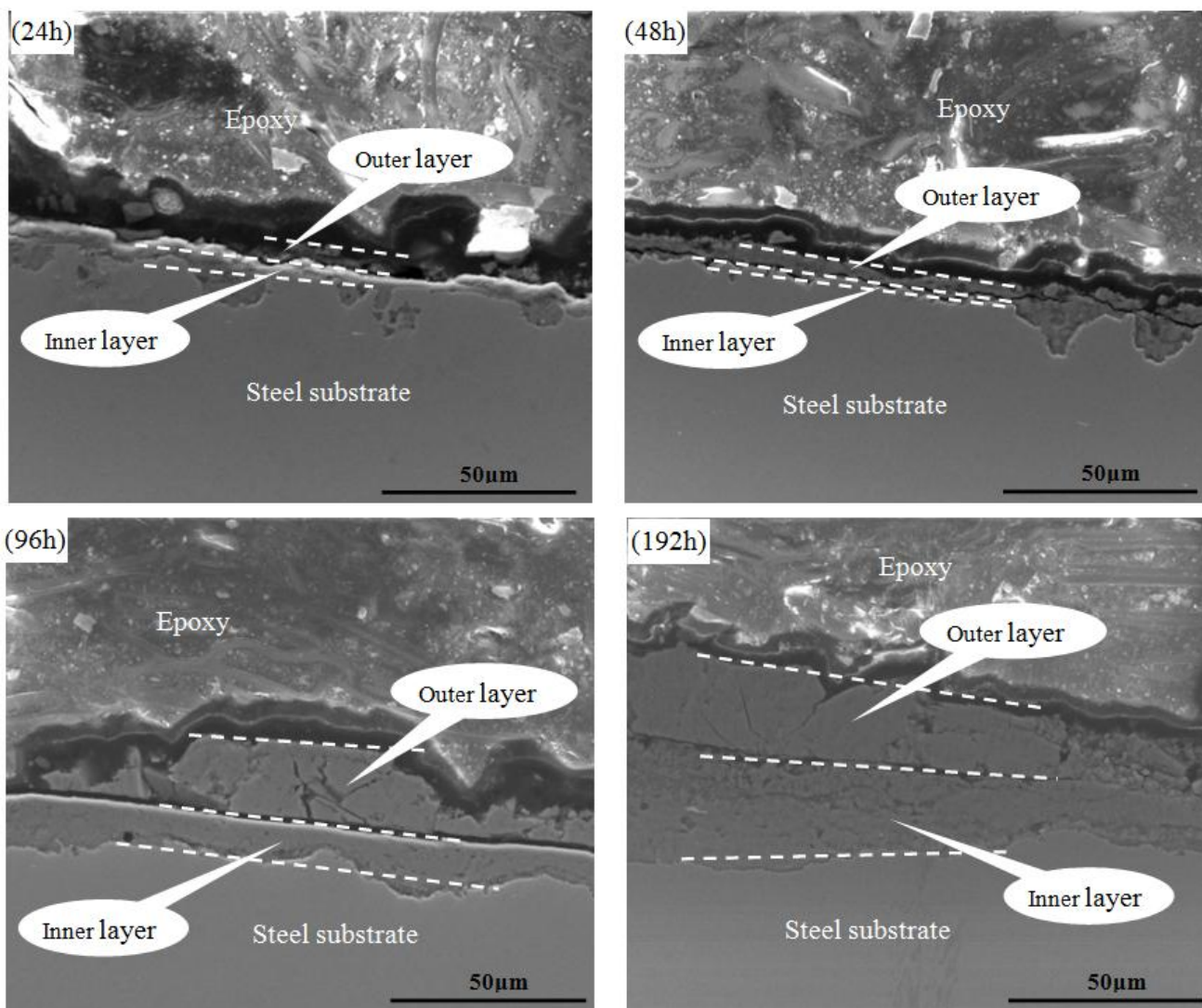
Figure 4. Cross-section morphology of different immersion durations

3.3 Electrochemical measurement analysis

3.3.1 Polarization curve analysis

Electrochemical measurement is considered to be a fast and efficient method which indicates the transient electrochemical process. The shape of polarization curve can obtain information on the

kinetics of the corrosion reactions. Potentiodynamic polarization measurement is conducted on the samples after different immersion period for 24 h, 48 h, 96 h and 192 h. The typical polarization curves are shown in Fig.5. The fitted values of corresponding kinetic parameters such as anodic and cathodic Tafel slope (ba, bc), corrosion potential (E_{corr}) and corrosion current densities (i_{corr}) are listed in Table1. It is seen that the largest corrosion current density is observed at immersion time for 48 h, and the smallest one is observed at immersion time for 192 h, which is in coincidence with the results of weight loss tests. Combining with the corrosion morphology Fig.2 and Fig.4, we can find the greater corrosion current density, the more serious matrix corrosion. Based on corrosion morphology analysis for 48 h, the through-thickness cracking destroy the corrosion product films, the electrolyte contacts with metal to form local corrosion, leading to increase the corrosion current density. It is found that the corrosion current density (I_{corr}) decrease with increase immersion from 48 h to 192 h, which can be attribute to the formation of intact passive films that provide very good protection for tested steel [26]. During the immersion time, the thickness of inner layer and outer layer increase, it will be beneficial to improve the corrosion resistance.
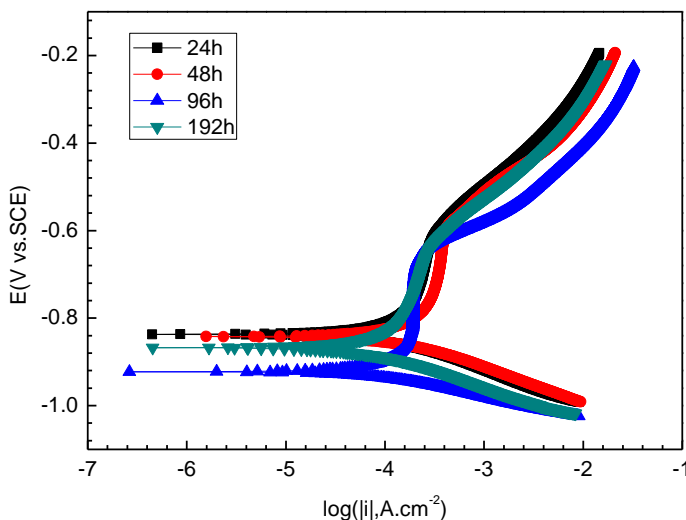
Figure 5. Potentiodynamic polarization curves of the tested steel after different immersion durations

Table 1. Potentiodynamic polarization parameters from a curve-fitting approach

Immersion time/hour	ba(mV/dec)	bc(mV/dec)	E_{corr}(mV vs.SCE)	i_{corr}(mA.cm^{-2})
24	998	-102	-837	0.187
48	920	-97	-842	0.258
96	881	-64	-923	0.143
192	485	-93	-868	0.116

3.3.2 EIS analysis

Electrochemical method is known to be an effective technology to study corrosion mechanism. The advantage of EIS is its ability to obtain information on corrosion processes that occur on the

electrode surface. For a better understanding of corrosion mechanism in sodium chloride solution containing H_2S and CO_2, the electrochemical impedance spectroscopy (EIS) measurement is performed under the same experimental conditions as the polarization curves. The typical Nyquist impedance diagrams during the early stages of corrosion for different immersion periods (24 h, 48h, 96 h and 192 h) are shown in Fig.6. We can see that each spectrum includes an incomplete of deformed semicircle. As immersion time increase from 48 to 192h, the diameter of semicircle at low frequency increases. The Bode diagrams are shown in Fig.7. As shown in Fig.7 (a), it is seen that the impedance modulus |Z| at the low frequency will gradually bigger with the increase immersion time, and the impedance modulus |Z| is biggest for tested steel after immersion 192 h, and the smallest one for immersion 48 h. As shown in Fig.7 (b), the broad-phase angle peak can show at least two time constants. So the electrochemical behavior can be simulated by a simple equivalent circuit in Fig.8. The dates are obtained from the equivalent circuits, which are listed in Table 2. In the circuit, Rs is the solution resistance. R_f is the resistance of corrosion product film. R_{ct} is the charge transfer resistance, which is used to represent the difficulty of the electrochemical reaction. CPE is the constant phase element representing the double-charge layer capacitance, which is expressed as follows.

$$Z_{CPE} = \frac{1}{Y_0 (j\omega)^n} \tag{4}$$

where Y_0 is a general admittance function, j is the complex operator with $j = (-1)^{1/2}$, $\omega = 2\pi f$ is the angular frequency, n is a power, which is an adjustable parameter that lies between 0 and 1. CPE_f represents total surface electrode capacitance after electrode surface dispersion, $n_1 (0 < n_1 < 1)$ is dispersion effect index of CPE_f, when $n_1 = 1$, CPE_f is equivalent to the ideal capacitance, when $n_1 = 0$, CPE_f is equivalent to the ideal resistance. CPE_{dl} represents the capacitance for solution/metal surface in the corrosion hole, $n_2 (0 < n_2 < 1)$ is dispersion effect index of CPE_{dl} [8].
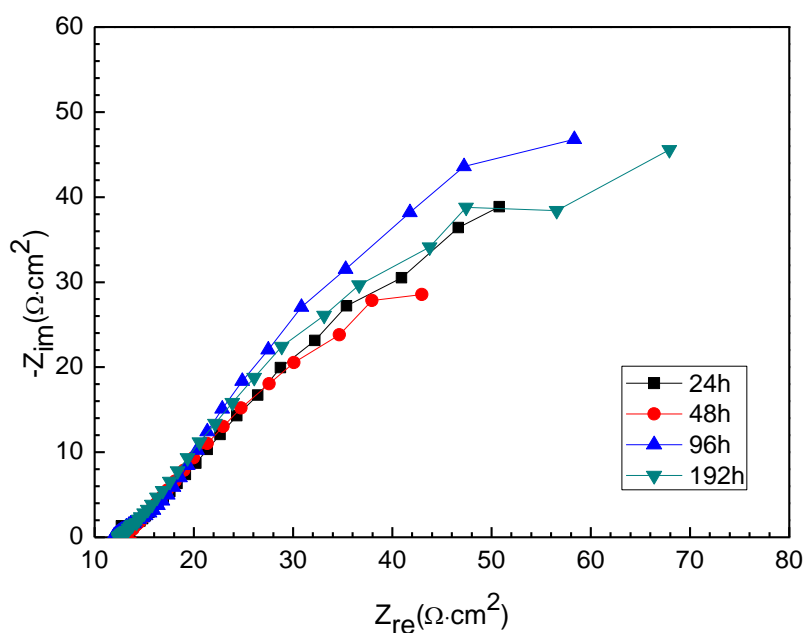
Figure 6. Nyquist plots of tested steel samples
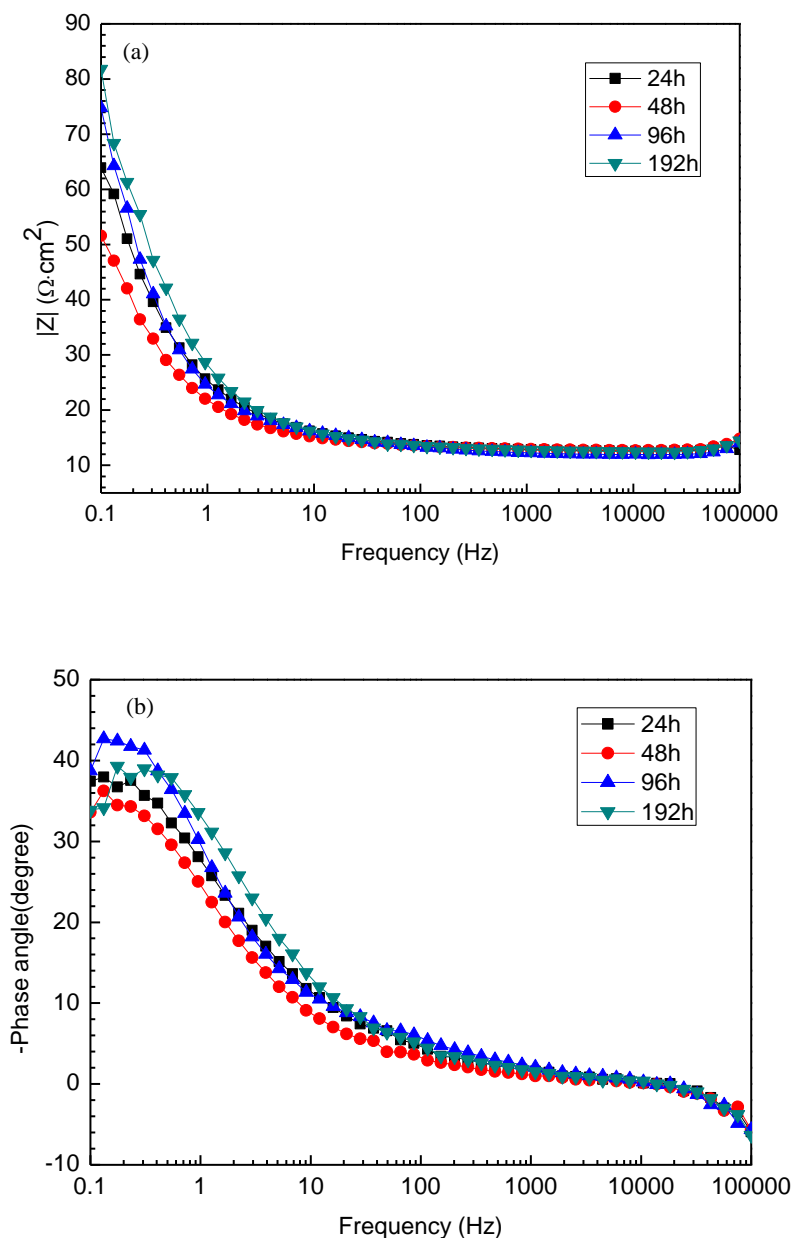
Figure 7. Bode diagrams of tested steel samples (a) The amplitude-frequency characteristic curve (b) The phase-frequency characteristic curve
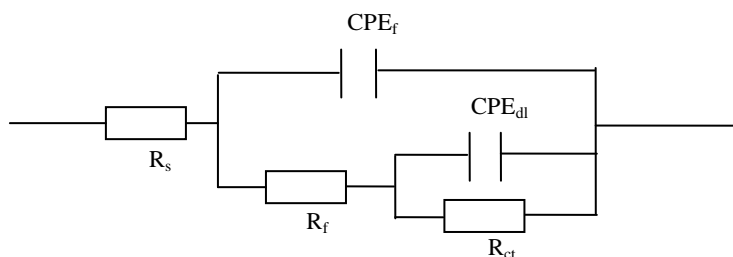
Figure 8. Equivalent circuits with two time constants

Table 2. The Parameters of equivalent circuit for tested steel

Immersion time/hour	R_s ($\Omega \cdot cm^2$)	Y_f ($\Omega^{-1}s^n cm^{-2}$)	n_1	R_f ($\Omega \cdot cm^2$)	Y_{dl} ($\Omega^{-1}s^n cm^{-2}$)	n_2	R_{ct} ($\Omega \cdot cm^2$)	R_{peis} ($\Omega \cdot cm^2$)	i_{eis} ($mA \cdot cm^{-2}$)
24	12.74	0.004624	0.7398	3.505	0.01675	0.6175	261	264.505	**0.152**
48	13.05	0.002813	0.6001	1.255	0.02816	0.6381	162	163.655	**0.233**
96	12.49	0.002106	0.5843	13.28	0.01534	0.6681	215	228.280	**0.114**
192	12.77	0.001497	0.9069	16.196	0.01352	0.6700	352	368.196	0.090

The relative residual errors for the real and imaginary components of the impendence (η_{re} and η_{im}) can be given using equations (5) and (6), respectively.

$$\eta_{re} = \left(\frac{Z_{re,\exp} - Z_{re,fit}}{Z_{re,\exp}} \right) \times 100\% \qquad (5)$$

$$\eta_{im} = \left(\frac{Z_{im,\exp} - Z_{im,fit}}{Z_{im,\exp}} \right) \times 100\% \qquad (6)$$

where $z_{re,\exp}$ and $z_{im,\exp}$ are the real and imaginary impedances measured from the EIS experimental results, respectively. $z_{re,fit}$ and $z_{im,fit}$ are the real and imaginary impedances obtained from the equivalent circuit. The errors with the exception of the highest frequency point are within 8%, it shows the effect of fitting is very good, the chosen equivalent circuit is correct.

We can see R_s changes a little from Table 2, the average value is about $12.76\,\Omega \cdot cm^2$, and the electrolyte resistance is almost the same, which will explain each test system is in a state of relative stability. With the increase immersion time, the resistances of corrosion product films (R_f) shows an increasing trend for immersion time from 48 to 192h, which may be result from the increase in film thickness. The polarization resistance from EIS can be expressed as $R_{peis} = R_{ct} + R_f$, which has been widely used to account for the kinetics of electrochemical corrosion [27-28]. The R_{peis} values will increase from 48 h to 288 h, the largest value is obtained for tested steel after immersion 192 h, the smallest one is obtained for immersion 48 h. R_{peis} is related to the corrosion current density i through the Tafel slopes anode slope b_a and cathode slope b_c according to Stern-Geary equation [29-30].

$$i_{eis} = \frac{1}{2.303 R_{peis} \left(\dfrac{1}{b_a} + \dfrac{1}{|b_c|} \right)} \qquad (7)$$

According to the equation (7), anodic and cathodic Tafel slope (ba, bc) in Table 1 and R_{peis} values in Table 2, the corrosion current density is calculated, as shown in Tables 2. The obtained result by the EIS is consistent with those obtained by weight loss and potentiodynamic polarization measurements.

4. CONCLUSIONS

The weight loss tests and electrochemical experiments are used to study the corrosion behavior and kinetics of early stages of low alloy steel under H_2S and CO_2 environment. The corrosion behavior is divided into three stages. At the first stage for immersion time before 48 h, a thin inner layer and a loose outer layer comprised of disperse mackinawite crystals appear on the sample surface. At the second stage from 48h to 96 h, a homogeneous mackinawite crystals are formed, the inner layer and the outer layer become denser and thicker. Finally, the protective films become more stably, some clusters of solid mackinawite are formed for immersion time 192 h, which will prevent the steel against corroding substrate further and improve the corrosion resistance.

References

1. W. He, O. Ø. Knudsen, S. Diplas, *Corros.Sci.*, 51(2009) 2811.
2. L.D. Paolinelli, T. Pérez, S. N. Simison, *Corros.Sci.*, 50(2008) 2456.
3. X. H. Hao, J. H. Dong, J. Wei, W. Ke, C. G. Wang, X. L. Xu, *Acta. Metall. Sin.,* 48(2012)534.
4. M.F. Wang, X.G. Li, N. Du, Y.Z. Huang, A. Korsunsky, *Electrochem. Commun.,* 10(2008) 1000.
5. F.U. Renner, A. Stierle, H. Dosch, D.M. Kolb, T.-L. Lee, J. Zegenhagen, *Nature,* 439(2006) 707.
6. L.Q. Guo, X.M. Zhao, B.C. Wang, Y. Bai, B.Z. Xu, L.J. Qiao, *Corros. Sc.,* 70 (2013)188.
7. A.M. Zimer, M.A.S. De Carra, E.C. Rios, E.C. Pereira, *Corros. Sci.,* 76 (2013)27.
8. P. P. Bai, S. Q. Zheng, C. F. Chen, *Mater. Chem. Phys.,* 149(2015)295.
9. E. Volpi, A. Olietti, M. Stefanoni, S. P. Trasatti, *J. Electroanal. Chem.,* 2015, 736(1): 38-46.
10. Y. Zou, J. Wang, Y. Y. Zheng, *Corros.Sci.,* 53(2011)208.
11. C. Yu, P. Wang, X. H. Gao, H. W. Wang, *Int. J. Electrochem. Sci.,* 10(2015)538.
12. S. Marcelin, N. Pébèr, S. Régnier, *Electrochim. Acta.,* 87(2013)32.
13. E. S. M. Sherif, A. A.Almajid, *Int. J. Electrochem. Sci.,* 10(2015)34.
14. L. W. Wang, C. W. Du, Z. Y. Liu, X. X. Zeng, X. G. Li, *Acta. Metall. Sin.,* 47(2011)1227.
15. G. A. Zhang, Y. Zeng, X. P. Guo, *Corros.Sci.,* 65(2012)37.
16. Y. G Zheng, J. Ning, B. Brown, S. Nešić, *Corros.,* 71(2015)316.
17. M. Liu, J. Q. Wang, W. Ke, E. H. Han, *J. Mater. Sci. Technol.,* 30(2014) 504.
18. Z. F. Yin, W. Z. Zhao, Z. Q. Bai, Y. R. Feng, W. J. Zhou, *Electrochim. Acta.*, 53(2008)3690.
19. F. L. Sun, X. G. Li, F. Zhang, *Acta. Metall. Sin.,* 26(2013)257.
20. A. K. Mishra, D. W. Shoesmith, *Corros.,* 70(2014)721.
21. L. Fan, D. H. Zhou, T. L. Wang, S. R. Li, Q, F, Wang, *Mater. Sci. Eng., A,* 590(2014)224.
22. C. Q. Ren, M. Zhu, L. Du, J. B. Chen, D. Z. Zeng, J. Y. Hu, T. H. S, *Int. J. Electrochem. Sci.,* 10(2015)4029.
23. W. F. Li, Y. J. Zhou, Y. Xue, *J. Wuhan. Univ. Technol. Mater.Sci.,* 28(2013)1038.
24. Y. M. Qi, H. Y. Luo, S. Q. Zheng, C. F. Chen, Z. G. Lv, M. X. Xiong, *Int. J. Electrochem. Sci.,* 9(2014) 2101.
25. G. Fierro, G. M. Ingo, F. Mancla, *Corros.,* 43(1989)814.

26. H. B. Li, Z. H. J, F. Hao, S. C. Zhang, P. D. Han, W. Zhang, G. P. Li, G. W. Fan, *Int. J. Electrochem. Sci.,* 10(2015) 4832.
27. A. V. C Sobral, W. Ristow, D. S. Azambuja, I. Costa, C. V. Franco, *Corros.Sci.*,43(2001)1019.
28. H. W. Wang, C. Yu, S. X. Wang, J. Gao, *Int. J. Electrochem. Sci.,* 10(2015)1169.
29. P. Qi, L. H. Jiang, H. Q. Chu, J. X. Xu, Y. Xu, *J. Wuhan. Univ. Technol. Mater.Sci.,*26(2011)1133.
30. E. McCafferty, *Corros.Sci.*, 47(2005) 3202.